NOTES AND CORRESPONDENCE

Some Evidence of Colinear Wind Stress and Wave Breaking

KARL F. RIEDER AND JEROME A. SMITH

Scripps Institution of Oceanography, University of California at San Diego, La Jolla, California

ROBERT A. WELLER

Woods Hole Oceanographic Institution, Woods Hole, Massachusetts

26 September 1995

ABSTRACT

Data collected during the Surface Waves and Processes Program are employed to investigate a possible interrelation between wind stress and surface wave breaking. From comparison of data from 15 half-hour long time segments, the directions of the wind stress and the whitecap motion are observed to be generally colinear, with both lying between the mean wind and the swell. As well, a nondimensionalized whitecap speed is found to correlate with the drag coefficient. These results suggest that the magnitude and direction of the wind stress might be estimated from wave breaking information.

1. Introduction

Energy for the growth of surface waves is provided by shear flows in the overlying atmospheric boundary layer. Recent work has shown that these shear flows are also altered by the underlying surface gravity waves; hence, the two are coupled (Geernaert 1990). In particular, wave direction has been shown to relate to the direction of the wind stress, which, in turn, does not necessarily align with the mean direction of the wind. The wind stress often veers toward the direction of the oblique swell (Geernaert et al. 1993; Rieder et al. 1994).

It has been found in laboratory experiments that wave breaking has a significant effect on the atmospheric boundary layer as well (Banner and Melville 1976; Melville 1977). Breaking waves are the location of airflow separation from the water surface and, hence, increase the phase shift between the air pressure at the surface and the wave elevation. Thus, wave breaking gives rise to significant "bursts" of momentum transfer (Banner 1990). An issue that has not been addressed in the laboratory, however, is whether the wind stress might relate to the direction of wave breaking versus the direction of the wind. This directional issue adds another dimension to the already perplexing uncertainty in estimating the stress magnitude.

A combination of data was collected during SWAPP (the Surface Waves and Processes Program), including measurements of the wind stress, surface waves, and wave breaking. These provide an opportunity to look into possible relations between breaking waves and wind stress. The surface wave and wave breaking data have been previously analyzed (Ding and Farmer 1994). They found that the mean direction of whitecap motion was generally aligned between the wind and waves; for cases in which the wind direction was significantly different from the direction of the waves, wave breaking was more closely aligned with the wind. Also, various measures of the degree of whitecapping (breaking event spacing, speed, dimension, and duration and active acoustic coverage) increased with wind speed. Here we introduce eddy correlation measurements of the wind stress, allowing us to address more directly interrelations of the wind, waves, breaking, and stress.

2. The experimental program and data analysis

SWAPP was designed for studies of interrelations between the wind, the heat flux, the waves, and the uppermost layers of the ocean (Weller et al. 1991). Data were collected from 24 February through 18 March 1990, from the Research Platform *FLIP*. The site was approximately 500 km off Point Conception, California, in a depth of 4000 m. Measurements of the surface gravity waves, mixed layer structure, and air–

Corresponding author address: Dr. Karl F. Rieder, Marine Physical Laboratory, Scripps Institution of Oceanography, University of California at San Diego, La Jolla, CA 92093-0213.
E-mail: krieder@opgl.ucsd.edu

sea fluxes were made. Other measurements, including those used to estimate wave breaking directions, were made from the Canadian vessel CSS *Parizeau*.

From *FLIP*, a four-beam, 195-kHz Doppler sonar system was used to estimate the directional wave spectra. A "quick-look" analysis of the measured surface velocities provides estimates of the first three Fourier components every 12.5 minutes within the frequency range of 0.05–0.5 Hz (Smith and Bullard 1995).

Two sonic anemometers were deployed on the aft and port booms of *FLIP* at 6 and 8 m above mean sea level, respectively. These measured the three components of wind speed and air temperature ten times per second, permitting calculation of the wind stress by the eddy correlation method:

$$\vec{\tau} = -\rho[\langle u'w'\rangle \mathbf{i} + \langle v'w'\rangle \mathbf{j}], \qquad (1)$$

where ρ is the water density and u', v', and w' are the downwind, crosswind, and vertical fluctuating air velocities. The sonic anemometer data were averaged and decimated to 2 Hz, and wind stress estimates were made every 30 minutes.

Air and sea temperatures and humidity were used to determine atmospheric stability (Large and Pond 1981). Atmospheric stability has been shown to influence the direction of the wind stress (Geernaert et al. 1993). For this study, only near-neutral conditions are considered, to separate the sea state influences from stability effects. Conditions are considered near-neutral here if $|z/L| < .05$, where z is the measurement height and L is the Monin–Obukhov length, a scale height for balancing buoyancy flux against wind stress.

To ensure well-defined wind and wind stress directions, the sonic anemometer data were required to satisfy several quality controls, as in Rieder et al. (1994): wind speeds of less than 3 m s^{-1} were not considered; estimates of the downwind stresses were required to be different from zero with a statistical confidence of 99%; and conditions during which the superstructure of *FLIP* sheltered or shadowed the sonic anemometer were removed. Only data from the sonic anemometer on the aft boom ever passed this last criterion.

The effect of sheltering is illustrated in Fig. 1. The directions relative to the aft boom of the wind (circles) and wind stress (crosses) are plotted versus the relative wind direction as given by a vector-averaging wind recorder (VAWR), mounted atop *FLIP* and not influenced by the superstructure. (Zero degrees indicates that the sonic anemometer is directly upwind of *FLIP*.) For wind directions such that the sonic anemometer was even partially in the lee of *FLIP*, unphysical stress directions are calculated. (The stress direction is more sensitive to sheltering than the wind direction, which appears reasonable for all cases shown here.)

The motion of *FLIP* was analyzed and found to be insignificant in producing errors in the wind stress calculation. For example, vertical and horizontal root-mean-square velocities of the sonic anemometer due to

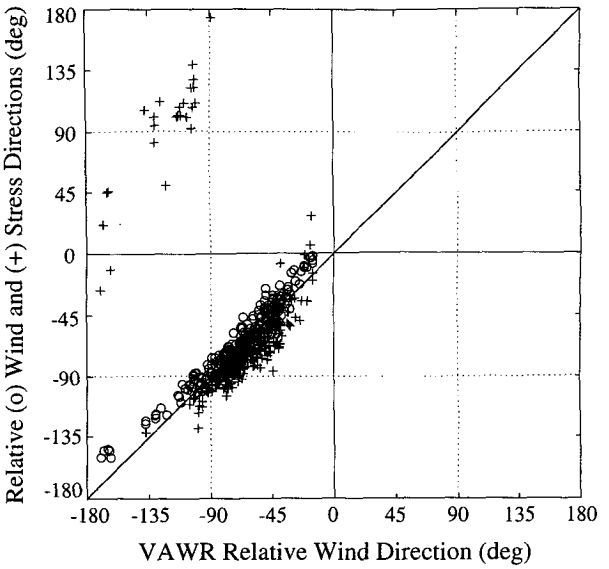

FIG. 1. Sonic-anemometer-measured wind and wind stress directions relative to the aft boom versus relative wind directions as measured by a vector-averaging wind recorder (VAWR) mounted atop *FLIP* (0 degrees indicates the sonic anemometer is directly upwind of *FLIP*). A strong influence on the wind stress direction can be seen for cases in which the sonic anemometer was even partially in the lee of the superstructure.

motion of *FLIP* are estimated at 0.03 and 0.15 ms^{-1}, respectively, for a representative sample period (20:29 March 11). However, the tilt and rotation of *FLIP* are independent, and the induced vertical and horizontal velocities are poorly correlated (correlation coefficient of $r^2 = 0.03$). The resultant wind stress contribution is estimated to be 8.8×10^{-4} N m^{-2}, more than two orders of magnitude smaller than the measured wind stresses.

Wave breaking data were collected and analyzed by Ding and Farmer (1994) from the *Parizeau*, stationed in the vicinity of *FLIP*. A drifting array of four hydrophones of span 8.5 m was deployed at 20-m depth to measure ambient sound produced by large-scale spilling breakers. Cross-correlations between hydrophones allowed construction of two-dimensional images, from which instantaneous locations of individual whitecaps were determined. These breaking events were tracked through time and breaking speed, direction, duration, and spacing were estimated. Mean values of these parameters were calculated over half-hour periods from between 300 and 500 breaking events (L. Ding 1994, personal communication).

Since each of these datasets (waves, wind, and breaking) were collected independently, it was necessary to find the time periods during which all of the measurements were made, and in which all data passed the selection criteria. Of the 23 half-hour time periods in which the wave breaking data are available, 3 had no sonic anemometer data, 3 failed the statistical con-

fidence criterion, and 1 had sheltering of both sonic anemometers behind *FLIP*'s superstructure. One of these also failed the near-neutral stability criterion. The remaining 15 time periods are shown in Fig. 2. The 6-m wind speed and wind and wave directions are plotted during the 10-day period in which the sonic anemometers were operational. The lines indicate the 15 periods for which all data were reported.

3. Wind stress and wave breaking

Figure 3 shows the directions of the mean wind, wind stress, swell, and wave breaking for the 15 half-hour time periods (numbered chronologically). The breaking direction is the mean direction of all breaking events (velocity weighted) for the period. The breaking event directions have a well-defined mean direction due to the large number of independent events (300–500 each half-hour). For the 15 cases analyzed here, mean breaking event directions could be determined to 99% confidence within ±1° on average and ±3° at worst (cf. Zar 1984). Similarly, mean stress directions were determined typically to ±1° and at worst to ±2°. Stress direction errors were made by first calculating the 99% confidence limits in the wind stress component perpendicular to the measured stress direction. The errors were then defined as the arc tangent of the ratio of these limits to the magnitude of the wind stress. Directions are plotted with the oceanographic convention, so 180° (for example) represents wind directed toward the

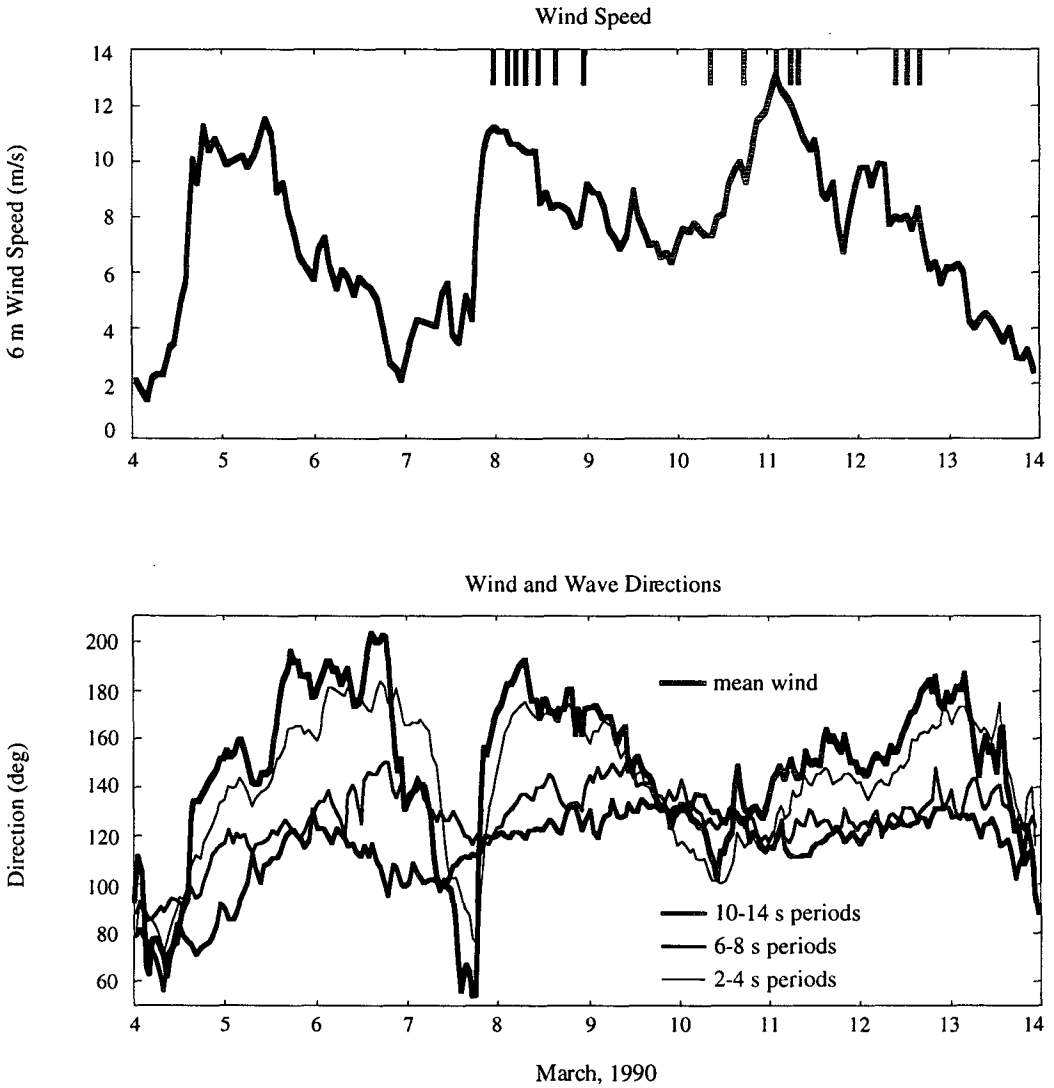

FIG. 2. Wind speed and wind and wave directions during SWAPP. Lines indicate half-hour time periods in which good wind stress, wave, and wave breaking data were all available. These 15 periods occurred only during the second and third wind events of the ten-day period.

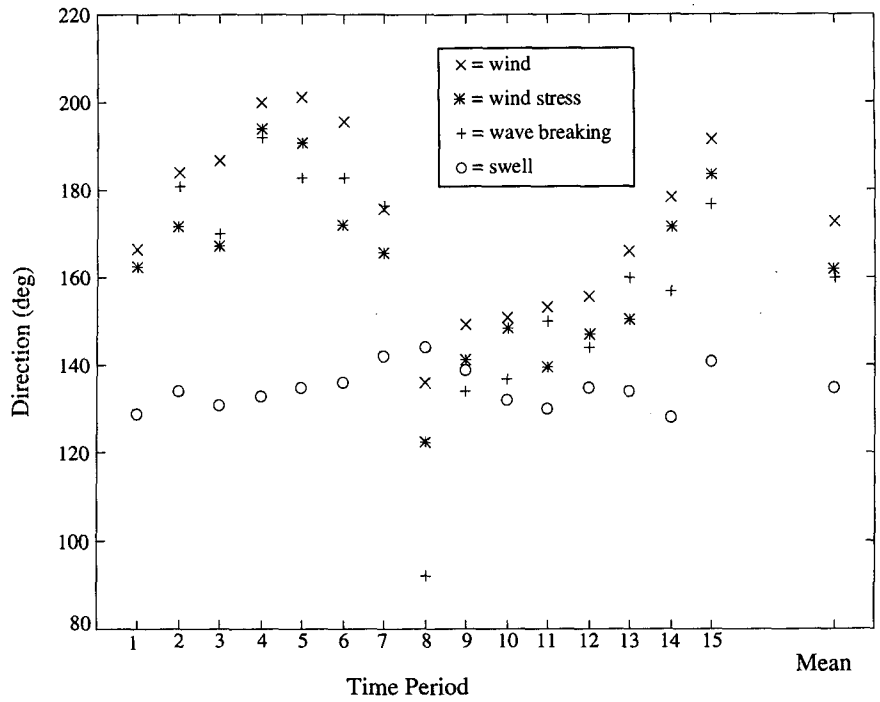

FIG. 3. Mean wind, wind stress, wave breaking, and swell directions for the 15 half-hour periods analyzed. Directions follow the oceanographic convention, for example, 180 indicates southward motion. For 13 of the 15 periods, both the wind stress and wave breaking are aligned away from the direction of the mean wind and toward the long period swell.

south. The wind was directed (Fig. 3) predominantly toward the SSE, and the swell to the ESE, with the two separated by 10° to 50°.

For all time periods except number 8 the wind stress was aligned between the mean wind and the swell, as reported by Rieder et al. (1994). For all but the eighth and ninth time periods, the mean direction of wave breaking was also between wind and swell. When there was a large angle between the wind and swell (time periods 1–7, 14, and 15), both wind stress and wave breaking were more closely aligned with the mean wind, whereas for small angles (time periods 8–13) the directions were more varied. The overall mean wind stress and wave breaking directions are very well aligned (Fig. 3, far right). The mean directions exhibit approximately 37° between the wind and swell, 11° between the wind and wind stress, and only 2° between the stress and wave breaking directions.

If we exclude time period 8, we find even better agreement between the mean wind stress and wave breaking directions, aligned within the accuracy of the measurements. Additionally, the mean square difference between wave breaking and wind stress directions is significantly reduced, from 132 to 75 deg^2. This can be compared to the mean square difference between wind and wind stress directions: 147 and 144 deg^2, including and excluding time period 8 respectively. The few hours surrounding period 8 are characterized by exceptionally large variability in the directions of wind, wind stress, and even waves. This might explain the anomalous results for this case.

With direct stress measurements, we can investigate also how the magnitude of the wind stress varies with wave breaking. Ding and Farmer (1994) showed that the degree of breaking, as measured by breaking event speed, dimension, spacing, or duration, increases with wind speed. Stress also increases with wind speed, as reflected in the concept of the drag coefficient: C_d is the coefficient of proportionality between the total wind stress magnitude and the square of the wind speed (this definition is consistent with inertial dissipation-method results). Thus, to reduce the overlap of information, we look for correlations between suitably normalized wave breaking parameters and the drag coefficient. Based on the measured 6-m drag coefficient versus nondimensional mean breaking event speed, defined as the mean whitecap speed divided by the 6-m height wind speed, a suggestion of a trend is seen in the data (Fig. 4a); however, the correlation coefficient squared of $r^2 = 0.18$ is below the 95% confidence level of $r^2 = 0.26$, based on the sample size of 15. However, if we exclude the anomalous time period 8, depicted by gray circles in Fig. 4, the correlation coefficient squared increases to $r^2 = 0.33$, well above the 95% confidence level. We also investigated breaking duration, dimension, and density; these display no stronger correlations

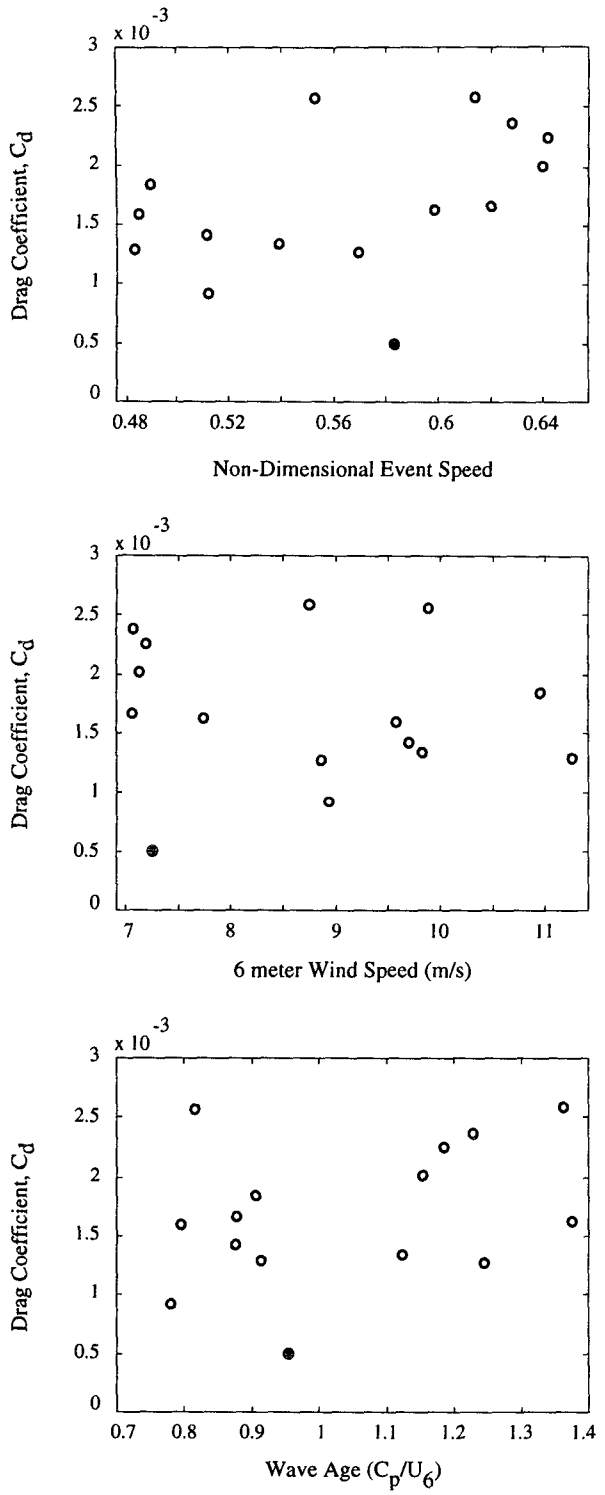

FIG. 4. Wind stress magnitude versus (a) dimensionless breaking event speed, (b) 6-m wind speed, and (c) wave age for the 15 half-hour periods analyzed. Gray circles represent anomalous time period 8. A trend of increased drag with increased dimensionless event speed is seen.

with the drag coefficient. For comparison, the drag coefficient is also shown versus the 6-m wind speed (Fig. 4b) and versus wave age (Fig. 4c). The wave age is a measure of the state of development of the seas. In order to avoid a spurious correlation with friction velocity, the wave age is defined here as the ratio of the phase speed of the peak sea frequency to the 6-m wind speed. Even though wind speed and wave age are the most commonly used parameters to model variations of the surface roughness, neither are found to correlate with the drag coefficient here ($r^2 < 0.11$), either including or excluding time period 8. Using just the downwind stress component in the calculation of the drag coefficient (as opposed to the total magnitude of the wind stress) slightly reduces the correlation with the nondimensional event velocity.

An alternate formulation is to ask whether wind stress can be estimated as well or better using only breaking event speed, as compared to using only wind speed. Indeed, from this limited dataset, we find a higher correlation of the wind stress with the square of the breaking event speed ($r^2 = 0.69$) than with the square of the wind speed ($r^2 = 0.42$). Testing whether these two correlations are statistically different from each other, we find (with the usual assumptions of normality, etc.) about two to one odds that breaking event speed does provide better estimates of the wind stress magnitude than wind speed, based on this small sample.

4. Discussion

Ding and Farmer (1994) noted that the wave breaking showed a general alignment between the wind and the waves. We now see that the wave breaking direction is more closely aligned with the wind stress direction than with either the wind or the waves alone. Also, Ding and Farmer showed correlations between measures of wave breaking intensity and wind speed; here we note a correlation with the wind stress, as well.

The overall alignment of wind stress and wave breaking directions and the correlation of the drag coefficient with a nondimensional breaking event speed suggest a connection between wave breaking and the wind stress. However, it does not suggest cause versus effect. On one hand, the input of momentum into the sea surface in a given direction may lead to preferential energy dissipation and wave breaking in that direction. As a large majority of the momentum transferred from the wind eventually goes to wave breaking, it should not be surprising for the wind stress and whitecapping to be aligned. On the other hand, the existence of wave breaking may produce a directional roughness effect and hence alter wind stresses, for example, via the mechanism described by Banner (1990). Finally, the observed alignment between the wind stress and wave breaking may be due to independent influences of the wind and waves on both these directions, and there may

not be any direct causal relationship between them. We emphasize that these results are purely observational and that the comparison with the works of Banner and Melville is only suggestive.

The alignment of stress and breaking directions is also interesting in light of previous findings. Geernaert et al. (1993) and Rieder et al. (1994) showed that the wind stress direction was influenced by the wave directions across a wide range of frequencies. While the spectral comparison of wave and wind stress directions addresses a continuous quasi-linear interaction between the wind and wave fields, the observed alignment of the wind stress and the wave breaking addresses an interaction that is episodic and conceptually highly nonlinear. This result draws attention to both the wide scale and varied nature of wind–wave coupling.

As a final note, these results suggest the possibility that the wind stress might be inferred from a subsurface, passive acoustic array: the magnitude and direction is obtained by finding the average speed and direction of wave breaking events. Such a system may offer some advantages over contemporary buoy-mounted systems, which are susceptible to motion-induced contamination, weathering, and encounters with surface vessels: the measurements may be carried out from a subsurface buoy or, in shallow water, from the sea floor. The technological development this would entail is worth considering.

Acknowledgments. Drs. Li Ding and David Farmer generously provided the wave breaking data. We particularly thank Dr. Ding for helping us interpret the data, and for his assistance in its reanalysis. We also thank Dr. Al Plueddemann for his help in the deployment of the sonic anemometers and Dr. Richard Seymour for his continued advice and support. This research was supported by the Office of Naval Research and the Mineral Management Service, under Contracts N00014-90-J-1285, N00014-93-1-0359, and N00014-93-1-1157.

REFERENCES

Banner, M. L., 1990: The influence of wave breaking on the surface pressure distribution in wind–wave interactions. *J. Fluid Mech.*, **211,** 463–495.

——, and W. K. Melville, 1976: On the separation of the air flow over water waves. *J. Fluid Mech.*, **77,** 825–842.

Ding, L., and D. M. Farmer, 1994: Observations of breaking surface wave statistics. *J. Phys. Oceanogr.*, **24,** 1368–1387.

Geernaert, G. L., 1990: Bulk parameterizations for the wind stress and heat fluxes. *Surface Waves and Fluxes.* Vol. 1. *Current Theory,* G. L. Geernaert and W. J. Plant, Eds., Kluwer Academic, 336 pp.

——, F. Hansen, M. Courtney, and T. Herbers, 1993: Directional attributes of the ocean surface wind stress vector. *J. Geophys. Res.*, **98,** 16 571–16 582.

Large, W. G., and S. Pond, 1981: Open ocean momentum flux measurement in moderate to strong winds. *J. Phys. Oceanogr.*, **11,** 324–336.

Melville, W. K., 1977: Wind stress and roughness length over breaking waves. *J. Phys. Oceanogr.*, **7,** 702–710.

Rieder, K. F., J. A. Smith, and R. A. Weller, 1994: Observed directional characteristics of the wind, wind stress, and surface waves on the open ocean. *J. Geophys. Res.*, **99,** 22 589–22 596.

Smith, J. A., and G. T. Bullard, 1995: Directional surface wave estimates from doppler sonar data. *J. Atmos. Oceanic Technol.*, **12,** 617–632.

Weller, R. A., M. A. Donelan, M. G. Briscoe, and N. E. Huang, 1991: Riding the crest: A tale of two wave experiments. *Bull. Amer. Meteor. Soc.*, **72,** 163–183.

Zar, J. H., 1984: *Biostatistical Analysis.* 2d ed. Prentice-Hall, 718 pp.